ORIGINAL ARTICLE

Fatigue Life Prediction for SiC/Al Materials Based on Path Planning Algorithm Considering Residual Stress

Wenqian Shang, Xintian Liu[*], Xu Wang and Xiaolan Wang

Abstract

To explore the influence of path deflection on crack propagation, a path planning algorithm is presented to calculate the crack growth length. The fatigue crack growth life of metal matrix composites (MMCs) is estimated based on an improved Paris formula. Considering the different expansion coefficient of different materials, the unequal shrinkage will lead to residual stress when the composite is molded and cooled. The crack growth model is improved by the modified stress ratio based on residual stress. The Dijkstra algorithm is introduced to avoid the cracks passing through the strengthening base and the characteristics of crack steps. This model can be extended to predict crack growth length for other similarly-structured composite materials. The shortest path of crack growth is simulated by using path planning algorithm, and the fatigue life of composites is calculated based on the shortest path and improved model. And the residual stress caused by temperature change is considered to improve the fatigue crack growth model in the material. The improved model can well predict the fatigue life curve of composites. By analyzing the fatigue life of composites, it is found that there is a certain regularity based on metal materials, and the new fatigue prediction model can also reflect this regularity.

Keywords Fatigue life estimation, Path planning, Residual temperature stress, Composite material

1 Introduction

Composites have been widely used in aerospace, machinery, shipbuilding and other fields [1]. Carbon fiber composites have good mechanical properties in various aspects, it is one of the most popular composite materials in our society today, and also need a more stringent working environment temperature compared to other composite materials [2], so excessive temperature will have a destructive effect on the material. Particle-reinforced metal materials are of isotropy, which is similar to metal materials, it has been mass-produced with different smelting technologies.

Materials will fail during working process, if a multiple cyclic stress far below the yield limit, it is defined as fatigue failure. The most failures are belong to fatigue failures in engineering program, and fatigue life prediction plays a significant role for reliability evaluation [3]. Failure occurrence is dangerous for both worker and product, it will lead to unnecessary economic losses in society. Therefore, it is important for the production to predict fatigue life of component more accurately [4–6]. The fatigue life prediction of traditional metal materials can be obtained by strength degradation model [7–9], damage accumulation model [10], energy method [11], S-N curve [12] and other methods [13, 14]. The fatigue life of materials will be affected by loading strength, load-stress ratio, and different load loading sequences [15–17]. In addition, the surface roughness and operating temperature of materials will also affect its fatigue life [18–20]. Many scholars have improved the model

*Correspondence:
Xintian Liu
xintianster@gmail.com
School of Mechanical and Automotive Engineering, Shanghai University of Engineering Science, Shanghai 201620, China

based on all these factors, and proposed many prediction methods considering material properties and working environment [21–23]. And some scholars analyzed the fatigue life by their numerical models [24–27]. Based on the research results of metal materials, scholars obtained fatigue life for metal matrix composites [28–30]. Metal matrix composites have better fatigue properties than metal alloys [31–34]. Fatigue or failure may be caused by these reasons, some people think that crack closure will be affected by the reinforcements of MMCs in crack propagation process [35, 36]. The fatigue life of MMCs is related to the increase in fatigue crack length and the reduction of the effective driving force for crack propagation caused by the deflection angle.

Path planning was originally part of preset algorithm of robot mobile behavior. According to some evaluation standard, an collision-free path can be found from the starting position to the target position in the obstacles environment [37]. The different distribution of these obstacles will affect the planned path in the environment. Path planning can be defined as an active behavior that allows a robot or mechanical device to find a path around an obstacle based on the environment. There is a variety of algorithms with different logic to be applied in path planning, such as Dijkstra algorithm, genetic algorithm, neural network algorithm [38], ant colony algorithm and so on. If the reinforcement particles of the material are distributed uniformly and disorderly, fatigue crack growth of particle-reinforced metal matrix composites will deflect or break through the reinforcement particles. Reinforcing particles hinder the growth of fatigue cracks, and the composite material has higher fatigue life than the metal in the macro. If the tip stress is large enough, the crack can go through the reinforcing particles. In an ideal condition, all the reinforcing particles can't penetrate, and crack growth and propagation can be prevented to the greatest extent, and MMCs will have higher life. The cracks bypass all reinforcing particles, and the behavior is similar to robot path planning. It is possible to predict the crack path by path planning algorithm. The fatigue behavior of composite materials is quite different from traditional metals. To predict MMCs' life more accurate, an improved fracture and fatigue crack growth (FCG) model is given by combining crack length and path planning algorithm.

2 Statement of the Problem

The fatigue life prediction of components is of great significance to product design and production safety. Composite materials have superior performance than traditional materials, which are replaced in some fields. The current prediction models are applied to obtain fatigue life of composite parts in a limited range. To predict the life of composite parts more accurately, the following issues should to be studied urgently:

(1) As a new type of material, the studies for composite materials are far less mature than the traditional, and the test data of composite materials are also less than common metals. It is very difficult to collect the parameters of composites than alloys, such as the strength, Poisson's ratio, and section shrinkage. There are many factors to affect the performance of composites, such as the reinforcing matrix volume fraction, metal-based alloy properties and the material manufacturing process. In summary, it is difficult for composite materials to reproduce the experimental data.

(2) There are different structures between composite materials and metals. Metal atoms are usually arranged in a certain shape, and some properties can be obtained. There are many forms of composite materials, and the ceramic particle reinforced metal matrix composites will be discussed. The composites are made of silicon carbide particles and alloys, and two materials can be connected by the interface. Due to the different microstructure, the internal stress distribution and fatigue crack growth of composite materials are totally different from the traditional metal.

(3) The fatigue failure mechanism of composite materials is different from traditional materials. Traditional prediction models are usually used to calculate fatigue life of the composites. Material performance parameters are replaced with composites, and rough estimates of fatigue life can be obtained. The crack fracture length can be expressed as follows:

$$a_c = \frac{1}{\pi}\left(\frac{K_{IC}}{F\sigma}\right)^2, \tag{1}$$

where a_c is the crack length when the material breaks, K_{IC} is fracture toughness, F is the shape factor, σ is the stress.

If it is necessary to calculate the crack fracture length of SiC/Al, the fracture toughness of SiC/Al can be replaced with Al. The force change is caused by the SiC reinforcing particles of the material, and the influence of force change is ignored to obtain the results. This method can be applied to deal with engineering problems within a certain range, and it is different to find the failure mechanism of the composite material.
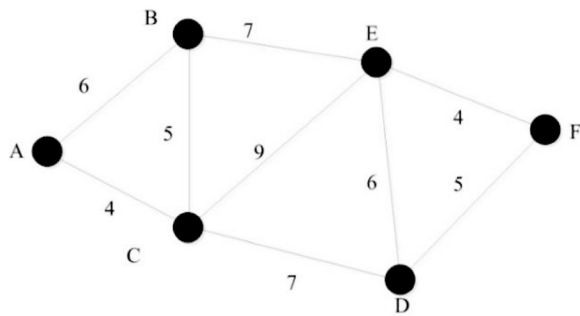
Figure 1 Schematic diagram of local shortest path

According to the failure process of composite materials, a new model is established to improve the accuracy of life prediction.

3 Crack Propagation Path Model

3.1 Dijkstra Algorithm

Dijkstra algorithm is used to simulate the path planning of random paths. This algorithm can be used to find the single-source shortest path of weighted directed graphs by breadth-first search. After many repetitions, the last shortest path will be found from the end point to the start.

The algorithm will be given to find the shortest path from the starting point A to the ending point F, and the schematic diagram of local shortest path can be shown in Figure 1. There are two arrays U and V, U indicates points that have been backtracked, V indicates points that have not been backtracked, and the number in parentheses is the shortest distance from point F. The process can be expressed as follows:

Step 1: U=[F(0)];
V=[D(5), E(4), C(∞), B(∞), A(∞)];
Step 2: U=[F(0), E(4)];
V=[D(5), C(13), B(11), A(∞)];
Step 3: U=[F(0), E(4), D(5)];
V=[C(12), B(11), A(∞)];
Step 4: U=[F(0), E(4), D(5), B(11)];
V=[C(12), A(17)];
Step 5: U=[F(0), E(4), D(5), B(11), C(12)];
V=[A(16)];
Step 6: U=[F(0), E(4), D(5), B(11), C(12), A(16)];
V=Ø.

According to step 2, the shortest distance between point C and F is 13, and the shortest path at this moment is (C, E, F). After an iteration, point D is added to the U array as the shortest path point. The shortest distance between point C and point F is 12, and the shortest path is changed to (C, D, F). After continuous iterations, the shortest path between two points can be obtained.

3.2 Random Barriers

SiC/Al composite material is made of aluminum alloy as the metal matrix, and SiC particles are evenly distributed in the metal matrix as a reinforcement. SiC particles are randomly distributed within a certain range on a microscopic scale, and their shapes are mostly random convex quadrilaterals. According to the composite characteristics, a model is established to simulate the distribution of random SiC particles.

If the crack propagation path extends to the position of the reinforcing base in the composite materials, the crack propagation path will deflect, and it will be lengthened. The rules of composite materials are different from the metals. It is easy to find the propagation path of cracks in composites, and the law of crack propagation is similar to robot path planning. The crack bypasses the reinforcement from the beginning to end, cracking rule is obtained by simulating the crack propagation path, and the relationship between the crack and the fatigue life will be obtained.

The reinforcement base is an irregular quadrangle and randomly distributed in the metal matrix. Supposing each quadrilateral is located as a cell, square interval is used in the path planning algorithm. If four random points are taken in a cell to represent the endpoints of the polygon, maybe the random quadrilateral formed with a "concave polygon". The "concave polygon" structure is prone to stress concentration at the shortest diagonal, and the reinforcing base particles often exist in the shape of "convex polygon" in practical engineering. In the modeling process, the strengthening basis is treated as a random quadrilateral, and the four endpoints fall into four square sub-regions that bisect the cell. Each sub-region is a grid, and points are randomly taken in each grid to form a random quadrilateral representing the position and shape of the reinforcing base. In composite materials, the reinforcing matrix is uniformly distributed in the metal matrix on a macroscopic scale. Based on microscopic observations, the spacing between particles is randomly distributed within a certain order of magnitude. The points are randomly taken from four adjacent grids with side length of 1.5 as the endpoint of the random quadrilateral, and its area size matches the actual particle size of 3–5 mm. During the modeling process, a random number is added to the cell distance. The coordinates of each
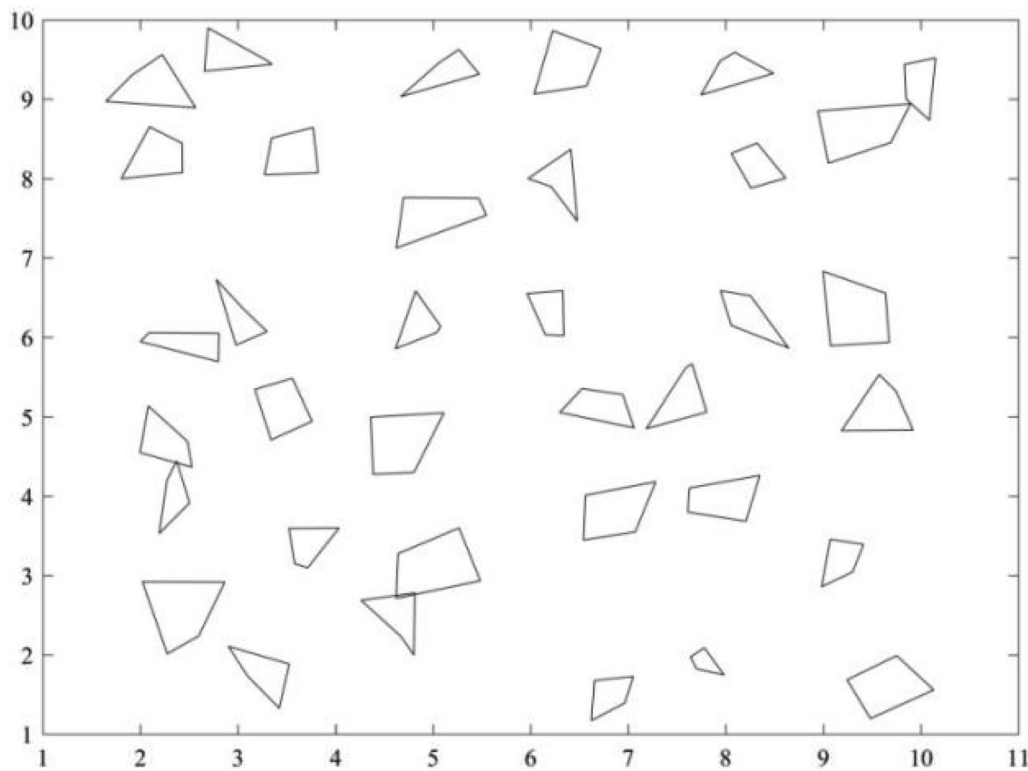
Figure 2 Random distribution of reinforcing base in matrix

endpoint for the random quadrilateral should to be stored in matrix A for subsequent calculations.

There is very little contact or even superposition between the reinforcing groups in Figure 2, and it can be considered as the phenomenon of reinforcing group polymerization in composite materials. The endpoint coordinates can be seen in Table 1.

3.3 Propagation Path Model

The midpoint of the line connecting the two adjacent quadrilateral endpoints is taken as the passable point, which can be given based on the position information of the random quadrilaterals. All possible paths for crack growth can be chosen from the line connecting these passable points. The coordinates of the passable points can be calculated from the data in matrix A, and the coordinates of each passable point are stored in matrix B.

After determining the starting point and the ending of the crack, the shortest crack is selected by the Dijkstra algorithm. Considering the ideal situation of the modeling, the stress intensity factors at the crack tip are not enough to break through the reinforcing base, and the path between the passing points must bypass the quadrilateral region. The connecting line of the passable points will be considered as possible path, the possible path can

not intersect any random quadrilateral edge. The rapid exclusion test and straddle experiment can be used to select the connecting lines. The validation can be given as follows.

A passable path and one side of the quadrilateral can be taken as an example, the line segment P_1P_2 is a passable path, and Q_1Q_2 is an edge of a quadrilateral. Suppose a rectangle with P_1P_2 as the diagonal, Q_1Q_2 is a rectangle made diagonally. The two line segments will not intersect as if the two rectangles are not intersect. If the two rectangles do not intersect, they will not pass the fast rejection experiment. If they fail to pass the fast rejection experiment, the two line segments will inevitably disjoin. If rapid rejection experiment is passed, a straddle experiment can be performed.

If a line segment P_1P_2 intersects with a line segment Q_1Q_2, then P_1P_2 is distributed at both ends of Q_1Q_2, that is straddle experiment. The logical relationship can be shown in Figure 3. It should be satisfied as follows:

$$\left((P_1 - Q_1) \times (Q_2 - Q_1)\right) * \left((Q_2 - Q_1) \times (P_2 - Q_1)\right) > 0, \tag{2}$$

where "$\times$" is the symbol of vector products, and "$*$" is the symbol of quantity products.

Shang *et al. Chinese Journal of Mechanical Engineering* (2023) 36:24

Page 5 of 12

Table 1 Obstacle endpoint matrix

	Column 1		Column 2		Column 3		Column 4		Column 5		Column 6	
Point 1	2.87	2.92	3.53	1.89	4.81	2.78	7.05	1.73	7.78	2.09	9.75	1.99
Point 2	2.02	2.92	2.90	2.11	4.26	2.69	6.65	1.68	7.64	1.97	9.24	1.69
Point 3	2.27	2.01	3.10	1.74	4.67	2.23	6.62	1.17	7.70	1.82	9.48	1.20
Point 4	2.60	2.24	3.42	1.33	4.80	2.00	6.96	1.39	7.98	1.75	10.13	1.56
Point 5	2.37	4.45	4.04	3.60	5.27	3.60	7.28	4.18	8.35	4.26	9.41	3.39
Point 6	2.27	4.20	3.52	3.60	4.64	3.28	6.56	4.01	7.63	4.10	9.07	3.46
Point 7	2.19	3.53	3.58	3.15	4.62	2.71	6.54	3.45	7.61	3.80	8.98	2.86
Point 8	2.50	3.92	3.71	3.10	5.49	2.94	7.07	3.55	8.21	3.69	9.30	3.05
Point 9	2.48	4.69	3.56	5.48	5.11	5.05	6.95	5.28	7.66	5.66	9.74	5.32
Point 10	2.08	5.14	3.17	5.34	4.36	5.00	6.53	5.35	7.59	5.62	9.57	5.53
Point 11	2.00	4.55	3.34	4.71	4.39	4.28	6.30	5.06	7.19	4.85	9.19	4.83
Point 12	2.53	4.37	3.76	4.95	4.80	4.30	7.06	4.86	7.80	5.06	9.92	4.84
Point 13	2.80	6.05	3.05	6.36	5.08	6.14	6.33	6.59	8.25	6.53	9.64	6.56
Point 14	2.09	6.06	2.78	6.73	4.82	6.58	5.96	6.55	7.95	6.59	9.00	6.83
Point 15	2.00	5.95	2.98	5.90	4.62	5.86	6.15	6.03	8.06	6.15	9.07	5.89
Point 16	2.80	5.69	3.30	6.07	5.04	6.06	6.34	6.02	8.64	5.87	9.68	5.94
Point 17	2.43	8.45	3.77	8.65	5.47	7.76	6.41	8.37	8.32	8.45	9.89	8.94
Point 18	2.09	8.65	3.35	8.51	4.70	7.76	5.97	8.00	8.06	8.32	8.94	8.85
Point 19	1.80	8.00	3.27	8.05	4.62	7.13	6.21	7.90	8.26	7.88	9.05	8.19
Point 20	2.43	8.08	3.82	8.08	5.55	7.54	6.48	7.46	8.61	8.01	9.69	8.45
Point 21	2.22	9.56	3.30	9.49	5.27	9.63	6.72	9.64	8.09	9.59	10.15	9.52
Point 22	1.91	9.31	2.69	9.90	5.06	9.46	6.23	9.86	7.94	9.49	9.83	9.44
Point 23	1.65	8.97	2.65	9.36	4.67	9.04	6.04	9.07	7.75	9.06	9.85	9.00
Point 24	2.57	8.89	3.35	9.44	5.47	9.32	6.57	9.17	8.49	9.33	10.09	8.74

The connection relationship between the passable points is stored in matrix *C*, which can be expressed as 1 and the unconnected is recorded as 0 for subsequent program calls, the connected matrix partial value are shown in Table 2. The Dijkstra algorithm will traverse all the paths between the set start and end points and find the shortest path through backtracking. The calculation results can be seen in Figure 4.

According to Figure 4, the crack needs to "bypass" the reinforcing base, and the crack will deflect without changing the overall direction. If the total length of the crack lengthens, the fatigue life of the composite material will be increased.

4 Fatigue Life Model

4.1 Residual Stress Model

The preparation temperature of the SiC / Al composite material is between 680° and 780°, and the material is cooled to normal temperature after the preparation. It will cause the change of material volume. Since the composite material is made of a mixture of metal and non-metal, the two materials have different expansion coefficients based on temperature, and residual stress will be generated during the cooling process. As shown in Figure 5, during the working process of the test piece, the residual stress will inevitably affect the stress ratio of the test piece.

The residual stress σ_α can be expressed as follows [37]:

$$\sigma_\alpha = \Delta\alpha\Delta t \frac{K_m K_i}{K_m + K_i}, \tag{3}$$

where $\Delta\alpha$ is the difference of expansion coefficients for the two materials, Δt is the difference between the preparation temperature and loading temperature, which fluctuates around 650°. K is the elastic modulus, the subscripts m and i are the matrix and the reinforcement, respectively.

The particle reinforced particles are added to the metal, and the stress field distribution can be shown in the composite in Figure 6. L is the length of the residual stress field. The existence of residual stress will affect the stress ratio of the load on the test piece.
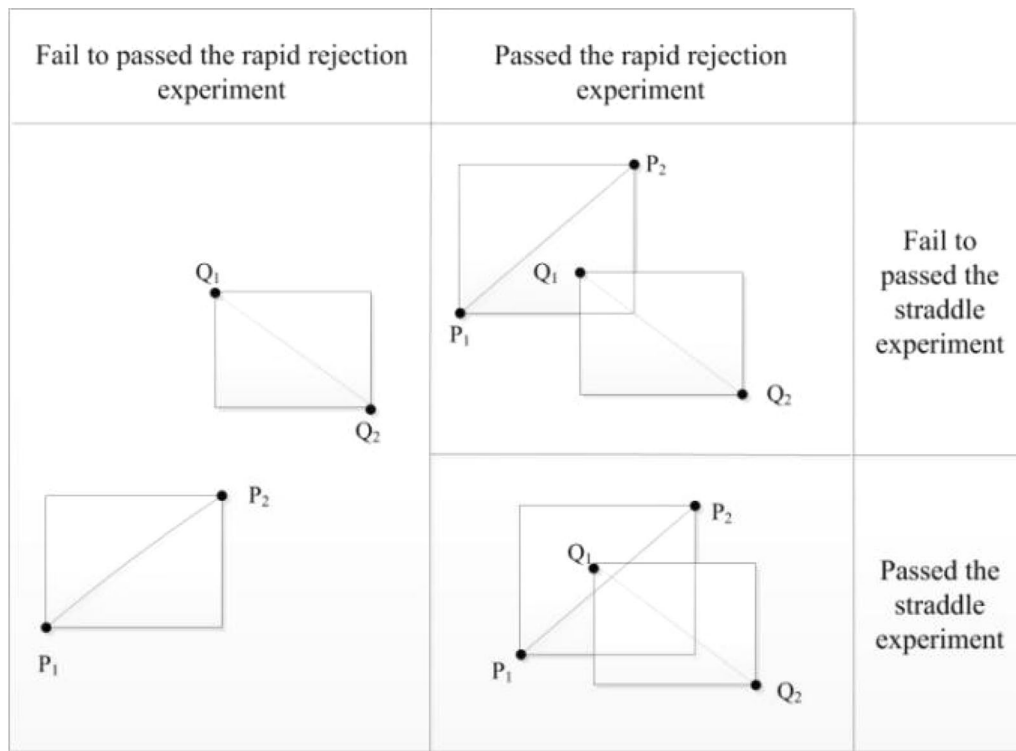
Shang *et al. Chinese Journal of Mechanical Engineering*   (2023) 36:24

Page 6 of 12

Figure 3 Diagram of intersection determination

Table 2 Connected matrix partial value

	1	2	3	4	5	6	7	8	9	10	11	12	13
1	0	0	1	0	1	1	0	0	0	0	0	0	0
2	0	0	1	0	1	1	0	0	0	0	0	0	0
3	1	1	0	0	1	1	1	1	0	0	0	0	0
4	0	0	0	0	0	0	0	0	0	0	0	0	0
5	1	1	1	0	0	1	1	1	1	0	0	0	0
6	1	1	1	0	1	0	1	1	1	0	0	0	0
7	0	0	1	0	1	1	0	1	1	0	0	0	0
8	0	0	1	0	1	1	1	0	1	0	0	0	0
9	0	0	0	0	1	1	1	1	0	0	0	0	0
10	0	0	0	0	0	0	0	0	0	0	1	1	1
11	0	0	0	0	0	0	0	0	0	1	0	0	1
12	0	0	0	0	0	0	0	0	0	1	0	0	1
13	0	0	0	0	0	0	0	0	0	1	1	1	0

According to the residual stress, the stress ratio R can be shown as follows:

$$R = \frac{\sigma_{\min} + \sigma_\alpha}{\sigma_{\max} + \sigma_\alpha}, \tag{4}$$

where $\sigma_{\min}$ is minimum stress, $\sigma_{\max}$ is maximum stress.

4.2 Initial Crack Model

The initial size of crack initiation should be determined and related to crack initiation life calculation. Crack initiation life N_i can be described as follows [39]:
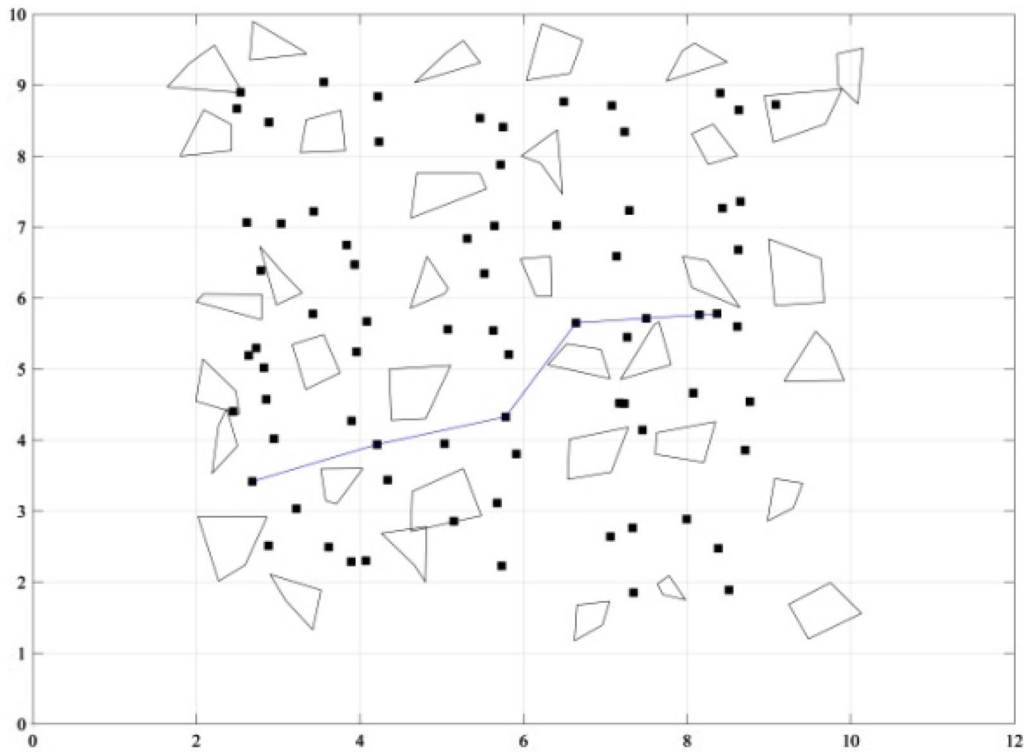
Shang *et al. Chinese Journal of Mechanical Engineering* (2023) 36:24

Page 7 of 12

Figure 4 Shortest path of crack propagation in composites

$$N_i = \left[\frac{2}{\varepsilon_f} \left(\frac{\Delta\sigma_{egv}^2}{EK} \right)^{\frac{1}{1+n}} - \frac{\Delta\varepsilon_c}{\varepsilon_f} \right]^{-2}$$

$$= \frac{1}{4} \left\{ \left(\frac{1}{EK\varepsilon_f^{1+n}} \right)^{\frac{1}{1+n}} \left[\Delta\sigma_{egv}^{2\frac{2}{1+n}} - \frac{\Delta\varepsilon_c}{2\varepsilon_f} \left(EK\varepsilon_f^{1+n} \right)^{\frac{1}{1+n}} \right] \right\}^{-2} \qquad (5)$$

$$= \frac{1}{4} \left(\frac{1}{E\sigma_f\varepsilon_f} \right)^{\frac{2}{1+n}} \left[\Delta\sigma_{egv}^{\frac{2}{1+n}} - \frac{\Delta\varepsilon_c}{2\varepsilon_f} \left(E\sigma_f\varepsilon_f \right)^{\frac{1}{1+n}} \right]^{-2},$$

where the fracture fatigue strength σ_f and the fracture fatigue strain ε_f are related to the reduction of area ψ, $\Delta\sigma_{egv}$ is equivalent stress, $\Delta\varepsilon_c$ is the threshold of strain range, E is elastic modulus, n is strain hardening exponent.

Equivalent stress $\Delta\sigma_{egv}$ can be given as follows:

$$\Delta\sigma_{egv} = \sqrt{\frac{1}{2(1-R)}} K_t \Delta\sigma, \qquad (6)$$

where K_t is the stress concentration factor and $K_t = 1$, $\Delta\sigma$ is stress amplitude.

The threshold of strain range $\Delta\varepsilon_c$ can be obtained as follows:

$$\Delta\varepsilon_c = \frac{2\tau_{-1}}{E} - \frac{\varepsilon_f}{10^{3.5}}, \qquad (7)$$

where τ_{-1} is torsional fatigue limit.

The fracture fatigue strain ε_f can be expressed as follows:

$$\varepsilon_f = -In(1-\psi), \qquad (8)$$

where ψ is reduction of area.

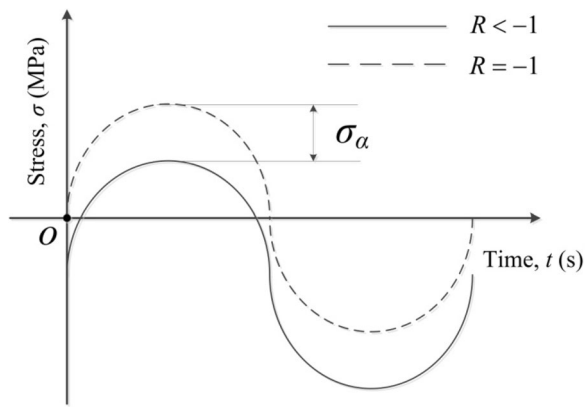The fracture fatigue strength σ_f can be calculated as follows:

Figure 5 The change of stress ratio related to residual stress

$$\sigma_f = \left(1 + In\frac{1}{1-\psi}\right)\sigma_b, \tag{9}$$

where σ_b is tensile strength.

The initial crack size a_0 can be given as follows:

$$a_0 = \frac{\left(K_{IC}/\sigma_b\right)^2}{\pi}. \tag{10}$$

Fracture toughness K_{IC} can be given as follows:

$$K_{IC} = 0.032E\sqrt{\pi n}. \tag{11}$$

4.3 Crack Growth Model

If a component is subjected to cyclic loads, fatigue cracks propagation will occur until the component begins to fatigue or fail. The relationship between crack length and propagation life can be constructed according to the Paris formula [40]:

$$\frac{\mathrm{d}a}{\mathrm{d}N_f} = C(\Delta K)^m, \tag{12}$$

where a is the crack length, N_f is the number of stress cycles, C and m are material coefficients, ΔK is stress intensity factor range,

$$\Delta K = F\sqrt{\pi a}(\sigma_{\max} - \sigma_{\min}). \tag{13}$$

To obtain the crack propagation life prediction more accurate, the Paris formula can be improved considering the stress ratio as follows [41]:

$$\frac{\mathrm{d}a}{\mathrm{d}N_f} = \frac{C(\Delta K)^m}{(1-R)K_c - \Delta K}, \tag{14}$$

K_c is stress intensity factor threshold.

According to Eq. (14), crack propagation life N_f can be expressed as follows:

$$N_f = \int_{a_0}^{a_c} \frac{[(1-r)K_c - \Delta K]\mathrm{d}a}{C\left(F\Delta\sigma\sqrt{\pi a}\right)^m}, \tag{15}$$
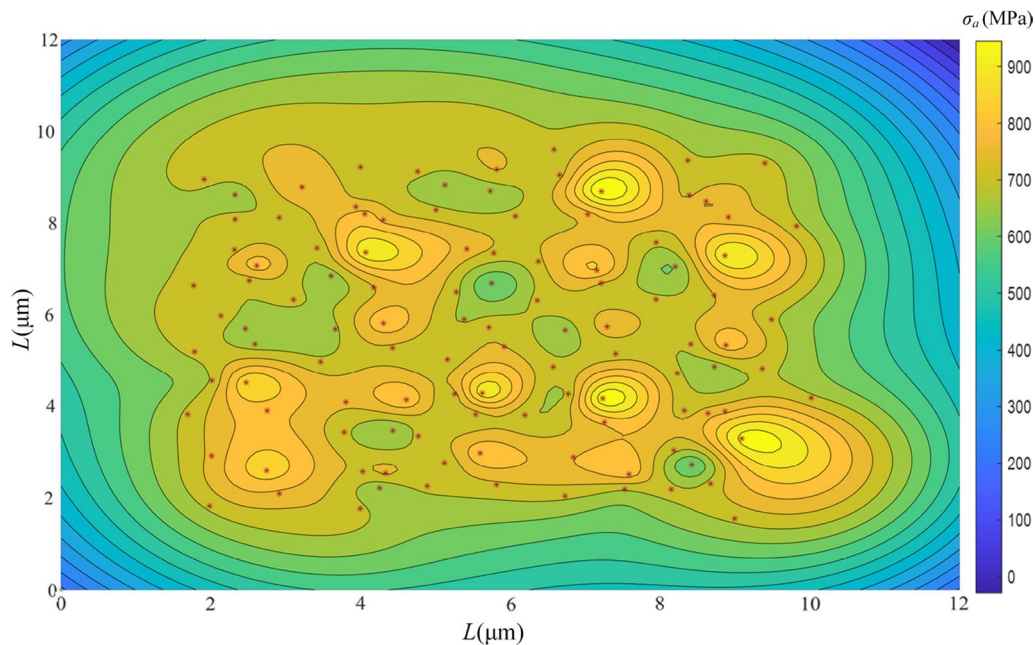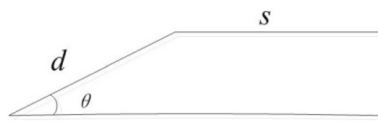

Figure 6 The contour field picture

Figure 7 Crack path deflection diagram

Table 4 Material properties of SiC/Al

Material	E (GPa)	δ_b (MPa)	$\delta_{0.2}$ (MPa)	ψ	P (C^{-1})
Al-20Si	89.1	361	309	0.1	24.2
SiC	450	–	–	–	3.4

Table 3 Composition of the Aluminum alloy (mass: %)

Material	Si	Mg	Cu	Mg	Mn	Al
Al alloy	20	0.3	0.116	0.3	0.116	remain

where a_c is the crack length in the material being broken.

Eq. (15) can be rewritten as follows:

$$N_f = \frac{(1-r)K_c}{C\left(F\Delta\sigma\sqrt{\pi}\right)^m\left(1-\frac{m}{2}\right)}\left(a_c^{1-\frac{2}{m}} - a_0^{1-\frac{2}{m}}\right)$$
$$- \frac{2}{C\left(F\Delta\sigma\sqrt{\pi}\right)^{m-1}(3-m)}\left(a_c^{\frac{3-m}{2}} - a_0^{\frac{3-m}{2}}\right). \tag{16}$$

A curve-fitted equation was given by Ref. [42] as follows:

$$\frac{\mathrm{d}a}{\mathrm{d}n} = \frac{C\left(1-f\right)^n\Delta K^n\left(1-\frac{\Delta K_{th}}{\Delta K}\right)^p}{(1-R)^n\left(1-\frac{\Delta K}{(1-R)K_c}\right)^q}, \tag{17}$$

where C, n, p and q are empirical constants, f is a crack-opening function empirical. The total life of the material is the sum of the initiation and extended life,

$$N = N_i + N_f. \tag{18}$$

When the crack path bends, the path direction deviates from the ideal crack direction, and the corresponding relationship between the crack length and the fatigue growth life also changes accordingly. The following equation can be modified as follows:

$$\frac{\mathrm{d}a}{\mathrm{d}n} = \alpha_1\left(\frac{\mathrm{d}a_1}{\mathrm{d}n}\right) + \alpha_2\left(\frac{\mathrm{d}a_2}{\mathrm{d}n}\right) + \ldots + \alpha_I\left(\frac{\mathrm{d}a_I}{\mathrm{d}n}\right)$$
$$= \sum_{i=1}^{I}\alpha_i\left(\frac{\mathrm{d}a_i}{\mathrm{d}n}\right), \tag{19}$$

$$\alpha = \frac{d\cos\theta + s}{d + s}, \tag{20}$$

where θ is the deflection angle, d is the distance to extend in the deflection direction, and s is the extension distance in the direction when the crack does not deflect. Crack path deflection can be seen in Figure 7.

If a deflection coefficient α_i are gotten in each possible path, all the deflection coefficient can be introduced into Eq. (20), the final crack propagation rate can be obtained.

5 Simulation Analyses

A model is proposed to predict fatigue life for metal matrix particle reinforced composites. To obtain the accuracy of the model, the test data in Ref. [43] is used for verification.

Composite material was produced and combined with a new type of aluminum alloy and SiC particles in Table 3 [43]. Table 4 shows the basic properties of the metal matrix. Material parameters C and m are equal to 7.8×10^{-4} and 0.09 respectively. Taking the material parameters into the life calculation model and giving different values to the fatigue stress, the fatigue life curve of Al alloy can be calculated, and it is as shown in Figure 8.

The S-N curve of Al-20Si metal is fitted by Eq. (19) as shown in Figure 8. It can be seen that most of the test value are close to the fitted curve. When the load is 140 MPa, there are some errors between the test result and curve. Ignoring experimental error factors, the load does not reach the fatigue expansion threshold, and leads to the actual life being longer than estimated life.

To calculate the fatigue life of composite materials, the stress ratio and path growth correction should be considered. As shown in Table 4, the coefficient of thermal expansion for Al alloy is 24.2×10^{-6}. The expansion coefficient of SiC particles is 3.4×10^{-6}. If the expansion coefficient of metal and nonmetal is brought into Eq. (3), the residual stress is -1.003×10^{-3}. Suppose the stress amplitude is 233 MPa, the original stress ratio is $r = 0.1$, and the modified stress ratio is $r = 0.7881$. The path correction value calculated by the path planning algorithm is 0.6650. Substituting the above values into Eqs. (16) and (18), the life curve of the composite can be obtained, and the comparison with the test results is shown in Figure 9. Figure 9 shows the relationship
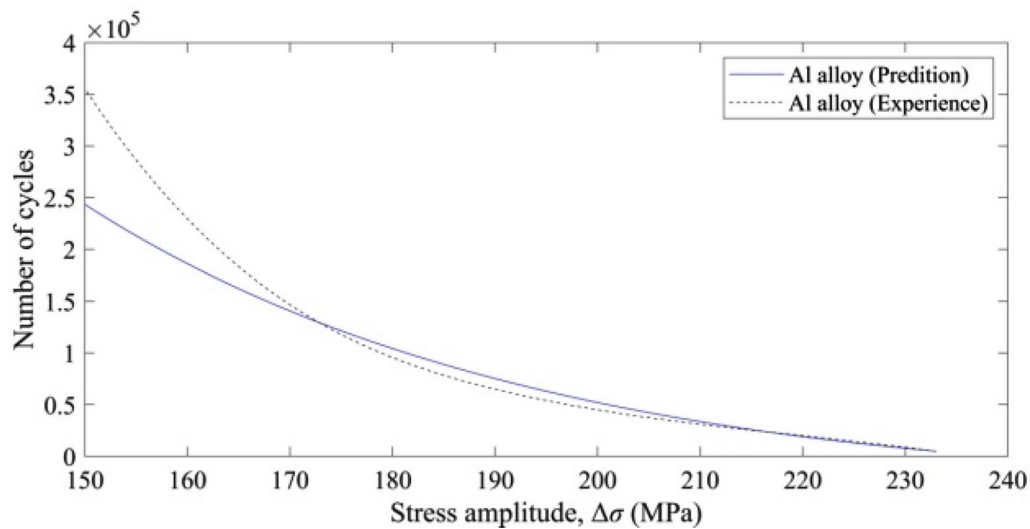
Figure 8 Comparison of experience data and fitting curve in Al alloy

between the calculated life curve of the composite material and the test results. The curve can be used to predict the life trend of experimental materials well. The tensile strength, elongation and other parameters of the metal matrix will change to varying degrees after adding the reinforcing base. Different from the regular fatigue life prediction method, crack deflection and residual stress are considered, and the change caused by the strengthening base is ignored in material properties. It can be seen from Figure 9, when the specimen is in a low stress environment, the new model data are not consistent with the experimental data very well, and the model is effective to obtain fatigue life in a certain extent.

According to Figures 8 and 9, when the stress level is 160 MPa, the error is the smallest in the predicted and the test life. When the stress level is higher than 160 MPa, the estimated life is higher than the test life, and the error increases with the increase of stress. Under very high stress levels, cracks will more easily penetrate the reinforced base without deflection. This process cannot be reflected by the life prediction model, and the test life will be larger than the calculation result which is not considered in penetrated condition. When the stress level is lower than 160 MPa, the predicted data is smaller than the test data. The presence of the reinforcement hinders the slip of the metal crystals, and will greatly increase the fatigue initiation life under small loads.

Based on this model, the path planning model can be used to analyze and discuss the composite fatigue life. The comparison of life increment for the two materials under different stresses is shown in Table 5.

It is easy to find that the increase of fatigue life of the composites reinforced by non-metallic particles conforms to a certain rule. The life prediction model of fatigue algorithm combined with path planning algorithm can reproduce this rule to a certain extent. The increase of fatigue life for composite materials decreases sharply in the region with large stress. The large fatigue stress destroys the non-metallic particles, and the path planning algorithm partially can used to simulate the failure.

6 Conclusions

Fatigue propagation characteristic of composite materials is studied, and a new model of the crack propagation path for composite materials is established according to the path planning algorithm. The differences between crack propagation length of composite and metal materials are estimated. The modified Paris model is used to estimate the fatigue life, and some conclusions can be drawn as follows:

(1) The crack trajectory simulated by the path planning model is closer to the microscopic crack trajectory, and the fatigue life is more accurately calculated using the estimated crack length. During regular fatigue failure of composite materials, the crack path will expand around the reinforcement base. The Dijkstra algorithm can effectively avoid the simulation of cracks passing through the strengthening base, and the local path optimization of the Dijkstra algorithm can be used to simulate the characteristics of crack "steps". This model can be extended to predict crack growth length for other similarly-structured composite materials.
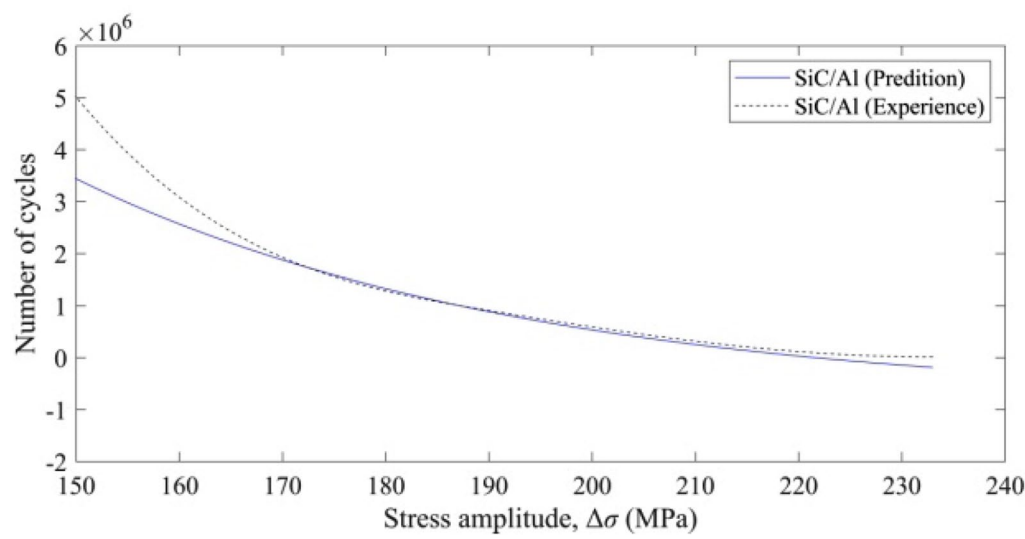
Figure 9 Comparison of experience data and fitting curve in SiC/Al composites

Table 5 Life increment of composite materials

Stress (MPa)	162		190		210	
	Exp	**Pre**	**Exp**	**Pre**	**Exp**	**Pre**
Al	210000	181246	65000	77878	31000	35237
SiC/Al	2800000	2493463	910000	928124	320000	280909
Change rate	13.33	13.76	14.00	11.91	10.32	7.97

(2) Considering the residual stress caused by temperature changing, the fatigue crack propagation model is improved. The residual thermal stress in the material is considered to improve the fatigue crack growth model.

(3) Based on the propagation of microscopic cracks, a new model of the life prediction for composite materials is presented. Combined with the crack length estimated by the path planning model, the fatigue crack propagation life is calculated. The experimental data show that the new model has some defects, and some works can be done in future.

Author contributions
Conceptualization and methodology were performed by XL and WS, data curation was performed by WS, supervision was performed by XL and XLW, reviewing and editing were performed by XW. The first draft of the manuscript was written by WS and all authors commented on previous versions of the manuscript. All authors read and approved the final manuscript.

Authors' Information
Wenqian Shang, born in 1994, is currently a master at *School of Mechanical and Automotive Engineering, Shanghai University of Engineering Science, China*. E-mail: shangwenqian@yeah.net.
Xintian Liu, born in 1980, is currently a professor at *School of Mechanical and Automotive Engineering, Shanghai University of Engineering Science, China*. He received his doctor degree from *University of Shanghai for Science and Technology, China*, in 2016. E-mail: xintianster@gmail.com.
Xu Wang, born in 1984, is currently a lecturer at *School of Mechanical and Automotive Engineering, Shanghai University of Engineering Science, China*.
Xiaolan Wang, born in 1985, is currently a lecturer at *School of Mechanical and Automotive Engineering, Shanghai University of Engineering Science, China*.

Competing Interests
The authors declare no competing financial interests.

Shang *et al. Chinese Journal of Mechanical Engineering*   (2023) 36:24

Page 12 of 12

References

[1] N Altinkok. Application of the full factorial design to modelling of Al_2O_3/SiC particle reinforced al-matrix composites. *Steel and Composite Structures*, 2016, 21(6): 1327−1345.

[2] K Fu, L Ye. Modelling of lightning-induced dynamic response and mechanical damage in CFRP composite laminates with protection. *Composite Structures*, 2019, 218: 162−173.

[3] R Masoudi Nejad, M Tohidi, A J Darbandi, et al. Experimental and numerical investigation of fatigue crack growth behavior and optimizing fatigue life of riveted joints in Al-alloy 2024 plates. *Theoretical and Applied Fracture Mechanics*, 2020, 108: 102669.

[4] R Liu, X J Wang, P W Chen, et al. The role of tension-compression asymmetrical microcrack evolution in the ignition of polymer-bonded explosives under low-velocity impact. *Journal of Applied Physics*, 2021, 129(17): 175108.

[5] S P Zhu, H Z Huang, W Peng, et al. Probabilistic physics of failure-based framework for fatigue life prediction of aircraft gas turbine discs under uncertainty. *Reliability Engineering & System Safety*, 2016, 146: 1−12.

[6] G Qian, M Niffenegger, M Sharabi, et al. Effect of non-uniform reactor cooling on fracture and constraint of a reactor pressure vessel. *Fatigue & Fracture of Engineering Materials & Structures*, 2018, 41(7): 1559−1575.

[7] M H Zhang, G Hu, X Liu, et al. An improved strength degradation model for fatigue life prediction considering material characteristics. *Journal of the Brazilian Society of Mechanical Sciences and Engineering*, 2021, 43(5): 275.

[8] S C Wu, Z W Xu, C Yu, et al. A physically short fatigue crack growth approach based on low cycle fatigue properties. *International Journal of Fatigue*, 2017, 103: 185−195.

[9] S C Wu, C H Li, Y Luo, et al. A uniaxial tensile behavior based fatigue crack growth model. *International Journal of Fatigue*, 2020, 131: 105324.

[10] X Liu, M H Zhang, H Wang, et al. Fatigue life analysis of automotive key parts based on improved peak-over-threshold method. *Fatigue & Fracture of Engineering Materials & Structures*, 2020, 43(8): 1824−1836.

[11] Q Wu, X Liu, Z Liang, et al. Fatigue life prediction model of metallic materials considering crack propagation and closure effect. *Journal of the Brazilian Society of Mechanical Sciences and Engineering*, 2020, 42(8): 424.

[12] M Wang, X Liu, X Wang, et al. Probabilistic modeling of unified S-N curves for mechanical parts. *International Journal of Damage Mechanics*, 2018, 27(7): 979−999.

[13] J Yu, S Zheng, H Pham, et al. Reliability modeling of multi-state degraded repairable systems and its applications to automotive systems. *Quality and Reliability Engineering International*, 2018, 34(3): 459−474.

[14] W Li, H Chen, W Huang, et al. Effect of laser shock peening on high cycle fatigue properties of aluminized AISI 321 stainless steel. *International Journal of Fatigue*, 2021, 147: 106180.

[15] J Gao, Z An, B Liu. A new method for obtaining P-S-N curves under the condition of small sample. *Proceedings of the Institution of Mechanical Engineers, Part O: Journal of Risk and Reliability*, 2017, 231(2): 130−137.

[16] R De Finis, D Palumbo, L M Serio, et al. Correlation between thermal behaviour of AA5754-H111 during fatigue loading and fatigue strength at fixed number of cycles. *Materials*, 2018, 11(5): 719.

[17] M Zhu, F Xuan. Fatigue crack initiation potential from defects in terms of local stress analysis. *Chinese Journal of Mechanical Engineering*, 2014, 27(3): 496−503.

[18] R Khan, R Alderliesten, S Badshah, et al. Effect of stress ratio or mean stress on fatigue delamination growth in composites: Critical review. *Composite Structures*, 2015, 124: 214−227.

[19] J de Krijger, C Rans, B Van Hooreweder, et al. Effects of applied stress ratio on the fatigue behavior of additively manufactured porous biomaterials under compressive loading. *Journal of the Mechanical Behavior of Biomedical Materials*, 2017, 70: 7−16.

[20] H Liu, H Liu, C Zhu, et al. Study on contact fatigue of a wind turbine gear pair considering surface roughness. *Friction*, 2020, 8(3): 553−567.

[21] D Cao, Q Duan, S Li, et al. Effects of thermal residual stresses and thermal-induced geometrically necessary dislocations on size-dependent strengthening of particle-reinforced MMCs. *Composite Structures*, 2018, 200: 290−297.

[22] X Liu, F Kan, H Wang, et al. Fatigue life prediction of clutch sleeve based on abrasion mathematical model in service period. *Fatigue & Fracture of Engineering Materials & Structures*, 2020, 43(3): 488−501.

[23] M H Zhang, X Liu, Y Wang, et al. Parameter distribution characteristics of material fatigue life using improved bootstrap method. *International Journal of Damage Mechanics*, 2019, 28(5): 772−793.

[24] Z You, X Liu, Z Jiang, et al. Numerical method for fatigue life of aircraft lugs under thermal stress. *Journal of Aircraft*, 2020, 57(4): 597−602.

[25] S P Zhu, Q Liu, J Zhou, et al. Fatigue reliability assessment of turbine discs under multi-source uncertainties. *Fatigue & Fracture of Engineering Materials & Structures*, 2018, 41(6): 1291−1305.

[26] J A F O Correia, A M P D Jesus, A S Ribeiro, et al. Strain-based approach for fatigue crack propagation simulation of the 6061-T651 aluminium alloy. *International Journal of Materials and Structural Integrity*, 2017, 11(1-3): 1−15.

[27] S K Josyula, S K R Narala. Study of TiC particle distribution in Al-MMCs using finite element modeling. *International Journal of Mechanical Sciences*, 2018, 141: 341−358.

[28] C R Ananth, N Chandra. Elevated temperature interfacial behaviour of MMCs: a computational study. *Composites Part A: Applied Science and Manufacturing*, 1996, 27(9): 805−811.

[29] W Li, H Liang, J Chen, et al. Effect of SiC particles on fatigue crack growth behavior of SiC particulate-reinforced Al-Si Alloy composites produced by spray forming. *Procedia Materials Science*, 2014, 3: 1694−1699.

[30] S Li, X Liu, X Wang, et al. Fatigue life prediction for automobile stabilizer bar. *International Journal of Structural Integrity*, 2020, 11(2): 303−323.

[31] H Z Ding, H Biermann, O Hartmann. A low cycle fatigue model of a short-fibre reinforced 6061 aluminium alloy metal matrix composite. *Composites Science and Technology*, 2002, 62(16): 2189−2199.

[32] G Costanza, R Montanari, F Quadrini, et al. Influence of Ti coatings on the fatigue behaviour of Al-matrix MMCs. Part I: fatigue tests and materials characterization. *Composites Part B: Engineering*, 2005, 36(5): 439−445.

[33] K Friedrich, A Fels, E Hornbogen. Fatigue and fracture of metallic glass ribbon/epoxy matrix composites. *Composites Science and Technology*, 1985, 23(2): 79−96.

[34] S H Lee, Y G Choi, S T Kim. Initiation and growth behavior of small surface fatigue cracks on SiC particle-reinforced aluminum composites. *Advanced Composite Materials*, 2010, 19(4): 317−330.

[35] J Ma, S Wang, C Meng, et al. Hybrid energy-efficient APTEEN protocol based on ant colony algorithm in wireless sensor network. *EURASIP Journal on Wireless Communications and Networking*, 2018, 2018(1): 102.

[36] Y Feng, M Zhou, G Tian, et al. Target disassembly sequencing and scheme evaluation for CNC machine tools using improved multiobjective ant colony algorithm and fuzzy integral. *IEEE Transactions on Systems, Man, and Cybernetics: Systems*, 2019, 49(12): 2438−2451.

[37] G Li, H Wang, Y Zhao, et al. High-temperature thermal expansion properties of Al_2O_3, Al_3Zr particulate reinforced Al-12%Si in situ matrix composites. *Chinese Journal of Engineering*, 2009, 31(5): 591−596. (in Chinese)

[38] B Yang, K Fu, J Lee, et al. Artificial neural network (ANN)-based residual strength prediction of carbon fibre reinforced composites (CFRCs) after impact. *Applied Composite Materials*, 2021, 28(3): 809−833.

[39] H Wang, X Liu, X Wang, et al. Numerical method for estimating fatigue crack initiation size using elastic-plastic fracture mechanics method. *Applied Mathematical Modelling*, 2019, 73: 365−377.

[40] P Paris, F Erdogan. A critical analysis of crack propagation laws. *Journal of Basic Engineering*, 1963, 85(4): 528−533.

[41] R G Forman, V E Kearney, R M Engle. Numerical analysis of crack propagation in cyclic loaded structures. *Journal of Basic Engineering*, 1967, 89(3): 459−463.

[42] R G Forman, S R Mettu. Behavior of surface and corner cracks subjected to tensile and bending loads in Ti-6Al-4V alloy. *Proceedings of the 22nd National Symposium*, Atlanta, June 26−28, 1990: s−611.

[43] C Li, Z Chen, D Chen, et al. Research on high-cycle fatigue behavior of spray deposited SiC_p/Al-20Si composite. *Journal of Mechanical Engineering*, 2012, 48(10): 40−44. (in Chinese)